NUCLEAR THEORY, Vol. 32 (2013)
eds. A.I. Georgieva, N. Minkov, Heron Press, Sofia

Relativistic Descriptions of Quasielastic Charged-Current Neutrino-Nucleus Scattering

G.D. Megias[1], **J.E. Amaro**[2], **M.B. Barbaro**[3], **J.A. Caballero**[1], **T.W. Donnelly**[4], **R. González-Jiménez**[1]

[1]Departamento de Física Atómica, Molecular y Nuclear, Universidad de Sevilla, 41080 Sevilla, Spain
[2]Departamento de Física Atómica, Molecular y Nuclear and Instituto Carlos I de Física Teórica y Computacional, Universidad de Granada, 18071 Granada, Spain
[3]Dipartimento di Fisica, Università di Torino and INFN, Sezione di Torino, Via P. Giuria 1, 10125 Torino, Italy
[4]Center for Theoretical Physics, Laboratory for Nuclear Science and Department of Physics, Massachussets Institute of Technology, CAmbridge, MA 02139, USA

Abstract. We compare the predictions of the SuperScaling model for charged-current quasielastic muonic (anti)neutrino scattering from ^{12}C with experimental data spanning an energy range up to 100 GeV. The sensitivity of the results to different parametrizations of the nucleon vector and axial-vector form factors and the differences between electron and muon (anti)neutrino cross sections relevant for the νSTORM facility are also discussed.

1 Introduction

The recent data on charged-current quasielastic (CCQE) muonic neutrino and antineutrino cross sections on a ^{12}C target measured by the MiniBooNE Collaboration at Fermilab [1, 2] for neutrino energies in the 1 GeV region, have led to an important debate concerning the relevance of the reaction ingredients: final-state interactions (FSI), low-lying nuclear excitations, effects beyond the impulse approximation (IA), *etc.*. The results have stimulated many theoretical studies [3–11] that attempt to explain the apparent discrepancy between the data and traditional nuclear models, such as the Relativistic Fermi Gas (RFG), RPA calculations, relativistic Green's function approaches and Relativistic Mean Field (RMF) theory.

An empirical solution to this puzzle, proposed by the MiniBooNE collaboration, advocates a value of the nucleon axial-vector dipole mass ($M_A \simeq 1.35$ GeV/c^2) [1] larger than the standard value ($M_A = 1.032$ GeV/c^2). On the other hand microscopic explanations based on multi-nucleon excitations, in particular two-particle emission, were proposed in [3, 4, 6, 9]. Those of [6, 9], although rather different in their basic ingredients, have been shown to give very good agreement with the MiniBooNE data, while those of [3, 4], which are based on the exact relativistic evaluation of the Meson Exchange Currents (MEC) within the 2p2h RFG approach, provide an enhancement of the cross sections but do not fully account for the discrepancy. It should be stressed that a consistent evaluation of the MEC contribution is technically hard to achieve and an exact relativistic gauge invariant calculation of both vector and axial-vector contributions to MEC in neutrino scattering is not yet available.

On the other hand, CCQE $\nu_\mu-$ and $\bar{\nu}_\mu-^{12}$C cross section measurements from the NOMAD collaboration [12] for higher beam energies, going from 3 to 100 GeV, do not call for an anomalously large axial-vector mass and do not appear to match with the lower-energy MiniBooNE results, as shown in Figure 1 where the two sets of data are displayed. It should also be mentioned that recent data on CCQE $\nu_\mu-$ and $\bar{\nu}_\mu-^{12}$C from the MINERνA Collaboration [13, 14] are claimed to disfavor the value $M_A \simeq 1.35$ GeV/c^2. It is thus desirable to perform a consistent theoretical analysis of the cross sections in the entire 0–100 GeV energy range, using a nuclear model which can be applied up to very high energies. Such a model must obviously fulfill two basic requirements: it has to be relativistic and it must successfully describe quasielastic (QE) electron scattering data from intermediate up to very high energies.

The SuperScaling (SuSA) model, based on the superscaling function extracted from QE electron scattering data, does a reasonable job of satisfying both of the above requirements: it is fully relativistic and has been constructed using those data as input. On the one hand, its applicability may be questioned at very low energies (meaning by that, momentum transfers $q \leq 400$ MeV/c and energy transfers $\omega \leq 50$ MeV), where collective effects which violate scaling dominate. On the other hand, the SuSA approach can be safely extended up to very high energies, since it is based on (e, e') data in a range going from intermediate to high energies and momentum transfers [15–17].

In summary, the model gives a very good representation of all existing QE electron scattering data for high enough momentum and energy transfers, to the extent that *quasielastic* scattering can be isolated. Additionally, the same scaling approach has been shown to be very successful when extended to higher energies into the non-QE regime where *inelastic* contributions dominate [18]. However, it does not account for the typically $10 - 20\%$ scaling violations that occur mainly in the transverse channel and are associated with non-impulsive processes induced by two-body meson-exchange currents (MEC) (see [19–22]). These should therefore be added to obtain a representation of all of the contributions to the inclusive cross section in the relevant kinematical regions. Although our present modeling of 2p2h MEC contributions is robust when the momentum and energy transfers are sufficiently large, its validity in the low-q/low-ω region is questionable — work is in progress to correct this deficiency.

The SuSA model has been extensively described in previous work (see, e.g., [23]). In this paper we only summarize the basic ideas and focus on applying them to CCQE (anti)neutrino scattering from ^{12}C, comparing the results with the

MiniBooNE and NOMAD data. We also study the sensitivity of the cross section to different up-to-date parametrizations of the nucleon form factors entering the cross section, G_E, G_M and G_A, studying in particular the effects of a monopole parametrization for the axial-vector form factor. Finally, we present the SuSA predictions for electron neutrino and antineutrino cross sections, with particular reference to the νSTORM kinematical conditions [24].

2 Results

The basic idea of the SuSA approach to neutrino scattering is as follows. A phenomenological superscaling function, extracted from QE (e, e') data within a fully relativistic framework and embodying the essential nuclear dynamics, is multiplied by the appropriate charge-changing $N \rightarrow N$ weak interaction cross sections in order to obtain the various response functions contributing to the inclusive (ν_l, l) cross section, R_L, R_T and $R_{T'}$, each response being a combination of vector and axial-vector components (see [23] for details).

In Figures 1 and 2 we compare the MiniBooNE and NOMAD QE data on ^{12}C for ν_μ and $\overline{\nu}_\mu$ scattering, respectively, with the RFG and SuSA results using the standard value $M_A = 1.032$ GeV/c^2 for the nucleon axial-vector dipole

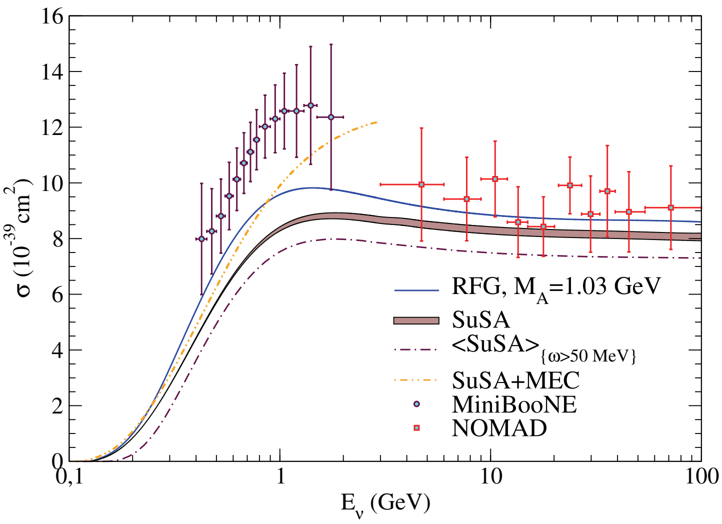

Figure 1. CCQE $\nu_\mu-^{12}$C cross section per nucleon displayed *vs.* neutrino energy E_ν and evaluated using the SuSA model (brown band) with the standard value of the axial-vector dipole mass $M_A = 1.032$ GeV/c^2. Results are also shown for the RFG model with $M_A = 1.032$ GeV/c^2 (blue solid curve) and compared with the MiniBooNE [1] and NOMAD [12] data. The MEC contributions are added to the SuSA model (orange dot-dot-dashed curve). Also presented for reference are the results for SuSA excluding all contributions coming from transferred energies below 50 MeV (dot-dashed curve).

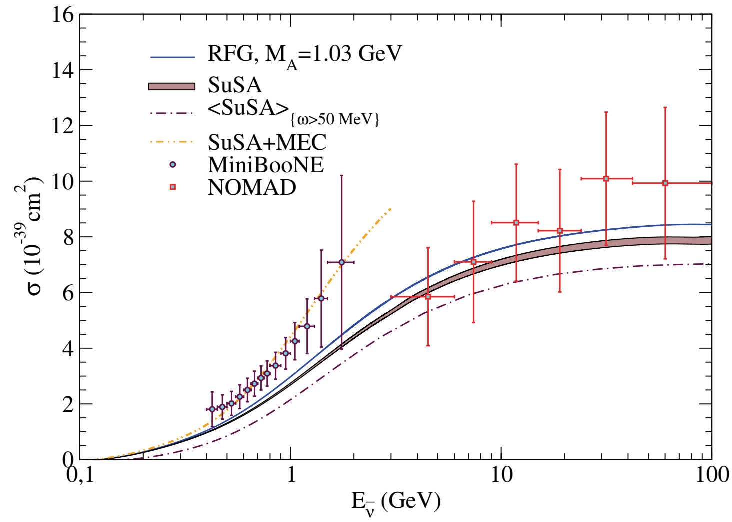

Figure 2. As for Figure 1, but now for $\overline{\nu}_\mu-{}^{12}$C scattering. MiniBooNE data are from [2].

mass. The SuSA results are represented by a narrow band, corresponding to the uncertainty linked to the use of two fits of the phenomenological scaling function [16, 17, 23]. We observe that the two models underestimate the MiniBooNE data for both neutrino and antineutrino scattering while they are both quite compatible with the NOMAD data. As already mentioned, this discrepancy could be solved by adding effects that go beyond the Impulse Approximation. In particular, as shown in Figures 1 and 2, the addition of MEC in the 2p2h RFG approach gives rise to results closer to MiniBooNE data, mainly for antineutrinos. It is important to point out that our present MEC parametrization is built solely from the pure vector transverse contribution, being applicable for neutrino energy values up to $1 - 1.3$ GeV. We pretend to extend the model to larger energies and incorporate a complete description of the MEC in the VA interference channel (essential to compute the T' response).

In order to clarify the relevance of each nuclear response, in Figure 3 we show the breakdown of the ν_μ and $\bar{\nu}_\mu$ cross sections into individual L, T and T' contributions, with the last occurring as a positive (constructive) term in the ν_μ cross section and a negative (destructive) term in the $\bar{\nu}_\mu$ cross section. Upon examining the results displayed in Figures 1 and 2 we note that were this VA interference is a bit larger, for instance via inclusion of contributions that go beyond the impulse approximation (see above), then better agreement with MiniBooNE data would be obtained, since this is where that term peaks, while the agreement with the antineutrino data could be less good. Some preliminary tests, including transverse MEC contributions with a soft raise in the T' response (10-15%), result in a very good agreement with MiniBooNE data for both ν_μ and $\bar{\nu}_\mu$ scattering.

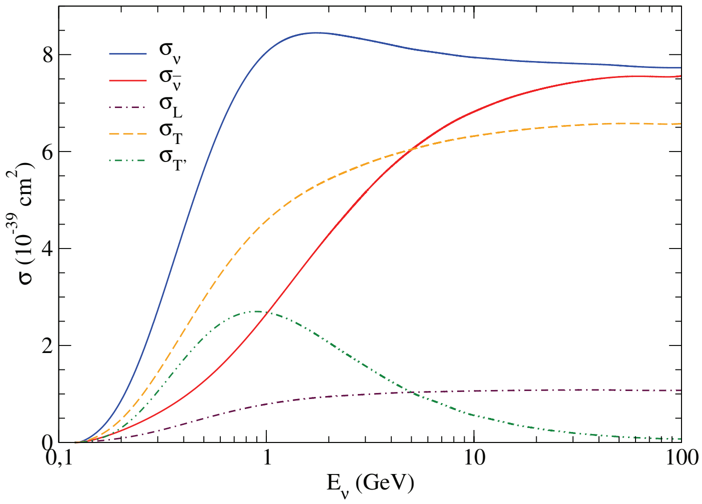

Figure 3. Separated L, T and T' contributions in the SuSA model.

We also present in Figures 1 and 2 the cross section computed with the SuSA model but where we have excluded all contributions coming from excitation energies below 50 MeV to assess the importance of this region in the total cross section. As can be seen, this region is quite important even for very high neutrino energies (typically amounting to about 10% of the total). As noted above, the SuSA approach was not formulated to deal with such low-energy excitations and one might be concerned that the present modeling is spurious for them. However, an alternative approach was taken long ago based on the excitation of discrete ph states in the regions up through where giant resonances dominate [25, 26] and encouragingly the present SuSA model and those old results essentially agree, giving us confidence that the SuSA approach on the average does a rather good job even at such low excitation energies. It should also be mentioned that in [27] the contribution of the discrete excitations of the final nucleus ^{12}N in CC neutrino scattering from ^{12}C was evaluated in a semi-relativistic shell model. The contribution from the discrete spectrum turned out to be below 2% for potential parameters fitted to reproduce the Q-value of the reaction.

In Figures 1 and 2 the electromagnetic form factors of the nucleon entering in the vector charged current are those of the extended Gari-Krumpelmann (GKex) model of [28–30], whose validity extends over a wide range in the transferred momentum. In Figure 4 we compare the SuSA results obtained with several other modern parametrizations of the form factors G_E and G_M [31]. In order to appreciate the dependence upon the vector form factors we do not show the error band in the SuSA result and instead have inserted a sub-panel zooming in on the region near the maximum. We observe that the uncertainties due to the electromagnetic nucleon form factors and the ones of the superscaling model are of the

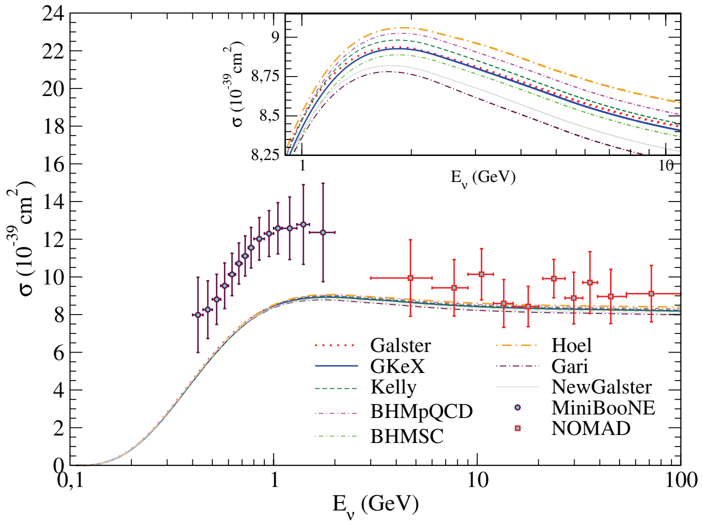

Figure 4. CCQE $\nu_\mu-{}^{12}$C cross section per nucleon evaluated in the SuSA model for various parametrizations of the nucleon electromagnetic form factors.

same order. Furthermore, all of the parametrizations are essentially equivalent for the kinematics that are relevant for these neutrino scattering experiments.

Next we explore the sensitivity of the cross sections to the axial-vector form factor. When employing a dipole parametrization for this the "standard" value of the axial-vector dipole mass is $M_A = 1.032$ GeV/c^2, whereas in analyzing the MiniBooNE data a large value of $M_A = 1.35$ GeV/c^2 was proposed [1]. The range spanned by these two is shown in Figure 5 for ν_μ and $\bar{\nu}_\mu$ scattering. Clearly the modified axial-vector mass produces an increase of the cross section that allows one to fit the low-energy data in the RFG model, although the increase is too large to explain the data at high energy. Although phenomenologically successful, the dipole parametrization cannot be justified from a field-theoretical point of view [32] and it is well-known, from vector-meson dominance (VMD) models, the fact that at moderate momentum transfers the EM magnetic form factors are roughly dipole-like is a conspiracy involving the (monopole) ρ and ω poles leading to an effective dipole behaviour, as discussed in [30]. Therefore, in addition to the standard dipole form, we also consider a monopole form $G_M^A(Q^2) = [1 + Q^2/\widetilde{M}_A^2]^{-1}$ motivated by VMD-based analyses such as those in [28, 29]. Using the range of monopole axial-vector masses $\widetilde{M}_A = 0.5 - 1.0$ GeV/c^2 considered in [31] and employing the SuSA model, we obtain the band shown in Figure 5. Note that increasing the axial-vector mass produces an increase of the cross sections with both parametrizations and a monopole axial-vector form factor with $\widetilde{M}_A \simeq 1$ GeV/c^2 leads to better agreement with both neutrino and antineutrino MiniBooNE cross sections.

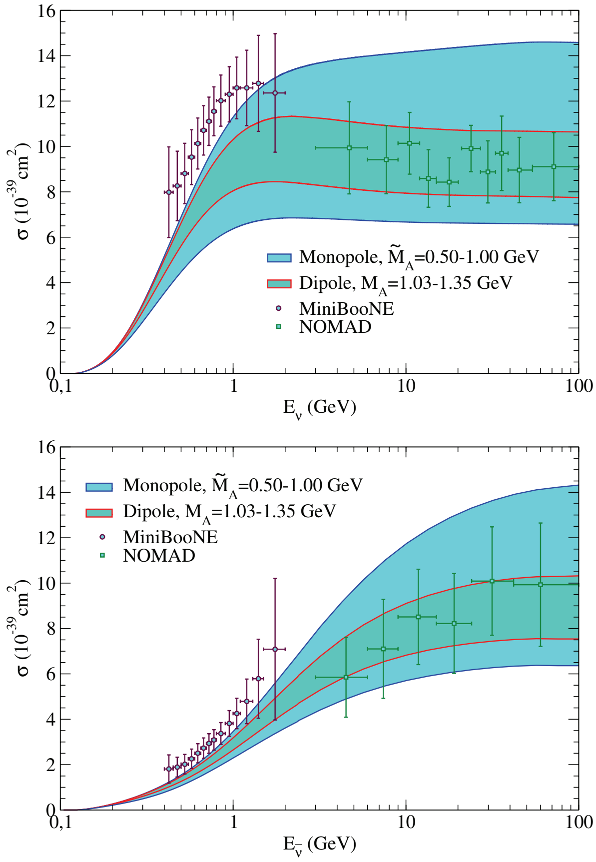

Figure 5. CCQE $\nu_\mu-{}^{12}$C (upper panel) and $\overline{\nu}_\mu-{}^{12}$C (lower panel) cross section per nucleon evaluated in the SuSA model for monopole (blue outer band) and dipole (red inner band) parametrizations of the nucleon axial-vector form factor. A larger mass yields a higher cross section.

On the contrary, the same model overestimates significantly the higher-energy NOMAD data. In fact, the band width linked to the two $\widetilde{M}_A$-values used with the monopole axial-vector form factor is much larger than the one corresponding to the dipole parametrization. This is in accordance with previous results shown within the framework of parity-violating electron scattering [31]. We should notice that a dipole axial-vector form factor with $M_A = 1.35$ GeV/c^2 (in the SuSA model) produces a cross section that is slightly lower in the MiniBooNE energy region than that obtained using $\widetilde{M}_A = 1$ GeV/c^2, but gives a "reasonable" explanation of the NOMAD data. On the other hand, $\widetilde{M}_A = 1$ GeV/c^2 is probably not a good choice because the neutrino cross section keeps rising even at high energies. Indeed if one were to accept the monopole parametrization and fit the

NOMAD data one would find that $\widetilde{M}_A = 0.70 \pm 0.06$ (0.72 ± 0.14) GeV/c^2 for ν_μ $(\overline{\nu}_\mu)$. Old experiments with deuterium bubble chambers also performed fits of the data using a monopole axial form factor obtaining $\widetilde{M}_A = 0.57 \pm 0.05$ [33] and $\tilde{M}_A = 0.54 \pm 0.05$ [34]. While these studies suggested that a dipole axial-vector form factor with the standard dipole mass is preferred, given the modern interest in a potentially different behaviour, especially at high momentum transfers, new studies of neutrino disintegration of deuterium would be very valuable in clarifying this issue.

Moreover, our interest is extended to the electron neutrino cross sections in order to compare the ν_e $(\overline{\nu}_e)$ and ν_μ $(\overline{\nu}_\mu)$ cross sections (see Figure 6) for the kinematics relevant for the proposed facility νSTORM [24], which will provide high quality electron neutrino beams in the energy range $E < 4$ GeV for precise measurements of neutrino-nucleus cross sections. In particular, this could allow one to study the differences between ν_μ and ν_e QE cross sections. Although the hadronic interaction is the same for ν_μ and ν_e, the different mass of the outgoing leptons produces a different energy transfer to the nucleus for the same incident neutrino energy, which results in a small shift for low neutrino energy. For higher energies the small differences due to the lepton mass tend to disappear, yielding a universal curve, independent of the neutrino flavour. As shown in [35] the RFG/SuSA models lead to almost identical results at energies above 1 GeV. On the contrary, for small energies one expects that the different nuclear excitation energy involved and the energy-dependence of the nuclear response functions will emphasize its differences. A precise measurement of the cross sections in this r

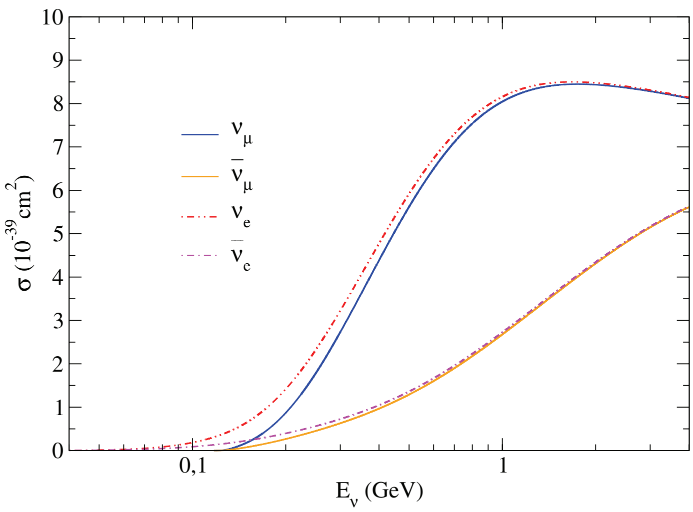

Figure 6. SuSA predictions for muon (solid curves) and electron (dotted curves) neutrino and antineutrino CCQE cross section per nucleon on ^{12}C.

electroweak nuclear matrix elements. Finally, another source of the difference between $\nu_e(\bar{\nu}_e)$ and $\nu_\mu(\bar{\nu}_\mu)$ cross sections comes from Coulomb corrections, *i.e.,* distortions of the final-state charged lepton wave functions in the Coulomb field of the nucleus, as described in [23]. Their effects, which are incorporated in all results shown in this work, become important only at neutrino energies below 200 MeV, where the cross sections are extremely small.

3 Conclusions

We have shown for the first time how the superscaling (SuSA) model behaves after being extended from intermediate to high energies as are relevant for recent neutrino scattering experiments. Note that, in spite of the slight differences between the RFG and SuSA predictions, smaller at high energies compared with the experimental error bars, the RFG fails to reproduce the (e, e') data, whereas the SuSA model agrees by construction with the electron scattering QE cross section. It is also remarkable that although the region of low excitation energy plays a significant role in the total cross section at all energies and consequently either of these models should be viewed with caution, since they are not well-suited to modeling the details of this region, in fact from comparisons with discrete-state modeling the SuSA approach does a reasonable job there when focusing on the total cross sections.

Whereas the SuSA model is expected to be robust enough to describe neutrino and antineutrino QE cross sections in all kinematic ranges, our present MEC parametrization lacks significant contributions: it is solely based on the pure transverse response and it fails in the region where the neutrino energy exceeds $\sim 1.3-1.5$ GeV. We are presently studying MEC contributions in the axial channel and its modeling to the low-q/low-ω region. We expect the new 2p2h MEC model to increase the low-neutrino-energy cross sections by $\sim 10-15\%$, but produce a negligible effect at higher energies. This will improve the description of all available data. Moreover, a different version of the SuSA approach, denoted as SuSAv2, is presently under way based on results provided by the RMF model. Contrary to SuSA, built solely from an universal superscaling function extracted from the analysis of the longitudinal (e, e') data, SuSAv2 is defined by taking into account the different nature of the longitudinal and transverse responses as well as the isovector/isoscalar channels involved in electron scattering reactions. Preliminary SuSAv2 results exhibit an enhancement of the total cross section ($\sim$15%), improving the comparison with data. This study will shortly be applied to MINERνA experiment.

We have presented cross sections for MiniBooNE and NOMAD conditions, employing the SuSA model to investigate several aspects of the neutrino-nucleus interaction entering into the cross section, namely the impact from vector and axial-vector nucleon form factors (monopole *vs.* dipole nature) and the dependence on the lepton flavour (at νSTORM kinematics). The axial-vector form factor determines the strength of the axial-vector current matrix elements and crucially depends on the value of the axial-vector mass parameter. The dependence of the cross section upon this parameter is significant and yields uncertainties that are bigger than the other model uncertainties for high energies.

Acknowledgements

This work was partially supported by DGI (Spain) grants FIS2011-28738-C02-01 and FIS2011-24149, by the Junta de Andalucia grants FQM-170 and FQM-225, by the Italian INFN under contract MB31, by the INFN-MICINN Collaboration agreement AIC-D-2011-0704, the Spanish Consolider-Ingenio 2000 programmed CPAN, and in part (TWD) by US Deptartment of Energy under cooperative agreement DE-FC02-94ER40818. GDM acknowledges support from the Fundación Cámara (University of Sevilla).

References

[1] A.A. Aguilar-Arevalo *et al.* [MiniBooNE Collab.], *Phys. Rev. D* **81** (2010) 092005.
[2] A.A. Aguilar-Arevalo *et al.* [MiniBooNE Collaboration], arXiv:1301.7067 [hep-ex]
[3] J.E. Amaro, M.B. Barbaro, J.A. Caballero *et al.*, *Phys. Lett. B* **696** (2011) 151.
[4] J.E. Amaro, M.B. Barbaro, J.A. Caballero *et al.*, *Phys. Rev. D* **84** (2011) 033004.
[5] J.E. Amaro, M.B. Barbaro, J.A. Caballero and T.W. Donnelly, *Phys. Rev. Lett.* **108** (2012) 152501.
[6] M. Martini, M. Ericson, G. Chanfray *et al.*, *Phys. Rev. C* **81** (2010) 045502.
[7] A.V. Butkevich, *Phys. Rev. C* **82** (2010) 055501.
[8] A. Meucci, M.B. Barbaro, J.A. Caballero *et al.*, *Phys. Rev. Lett.* **107** (2011) 172501.
[9] J. Nieves, I. Ruiz Simo and M.J. Vicente Vacas, *Phys. Lett. B* **707** (2012) 72.
[10] O. Lalakulich, K. Gallmeister and U. Mosel, *Phys. Rev. C* **86** (2012) 014614.
[11] J.T. Sobczyk, *Phys. Rev. C* **86** (2012) 015504.
[12] V. Lyubushkin *et al.* [NOMAD Collaboration], *Eur. Phys. J.* **C63** (2009) 355.
[13] L. Fields *et al.* [MINERvA Collaboration], arXiv:1305.2234 [hep-ex].
[14] G.A. Fiorentini *et al.* [MINERvA Collaboration], arXiv:1305.2243 [hep-ex].
[15] D. B. Day, J.S. McCarthy, T.W. Donnelly and I. Sick, *Ann. Rev. Nucl. Part. Sci.* **40** (1990) 357.
[16] T.W. Donnelly and I. Sick, *Phys. Rev. Lett.* **82** (1999) 3212.
[17] C. Maieron, T.W. Donnelly and I. Sick, *Phys. Rev. C* **65** (2002) 025502.
[18] C. Maieron, J.E. Amaro, M.B. Barbaro *et al.*, *Phys. Rev. C* **80** (2009) 035504.
[19] T.W. Donnelly, J.W. Van Orden, T. De Forest Jr. *et al.*, *Phys. Lett. B* **76** (1978) 393.
[20] J.W. Van Orden and T.W. Donnelly, *Ann. Phys.* **131** (1981) 451.
[21] A. De Pace, M. Nardi, W.M. Alberico *et al.*, *Nucl. Phys. A* **726** (2003) 303.
[22] J.E. Amaro, C. Maieron, M.B. Barbaro *et al.*, *Phys. Rev. C* **82** (2010) 044601.
[23] J.E. Amaro, M.B. Barbaro, J.A. Caballero *et al.*, *Phys. Rev. C* **71** (2005) 015501.
[24] P. Kyberd *et al.* [νSTORM Collaboration], arXiv:1206.0294 [hep-ex].
[25] J.S. O'Connell, T.W. Donnelly and J.D. Walecka, *Phys. Rev. C* **6** (1972) 719.
[26] T.W. Donnelly, *Prog. Part. Nucl. Phys.* **13** (1985) 183.

[27] J.E. Amaro, M.B. Barbaro, J.A. Caballero and T.W. Donnelly, *Phys. Rev. Lett*. **98** (2007) 242501.

[28] E.L. Lomon, *Phys. Rev. C* **64** (2001) 035204.

[29] E.L. Lomon, *Phys. Rev. C* **66** (2002) 045501.

[30] C. Crawford *et al.*, *Phys. Rev. C* **82** (2010) 045211.

[31] R. Gonzalez-Jimenez, J.A. Caballero and T.W. Donnelly, *Phys. Rept.* **524** (2013) 1.

[32] P. Masjuan, E. Ruiz Arriola and W. Broniowski, *Phys. Rev. D* **87** (2013) 014005.

[33] N.J. Baker, A.M. Cnops, P.L. Connolly *et al.*, *Phys. Rev. D* **23** (1981) 2499.

[34] K.L. Miller, S.J. Barish, A. Engler *et al.*, *Phys. Rev. D* **26** (1982) 537.

[35] G.D. Megias, J.E. Amaro, M.B. Barbaro, J.A. Caballero and T.W. Donnelly *Phys. Lett. B* **725** (1972) 170-174.